Graphite/MnO_2 and MoS_2 Composites Used as Catalysts in the Oxygen Reduction Cathode of Microbial Fuel Cells

Bolong Jiang,[a,z] Thorben Muddemann,[a,b] Ulrich Kunz,[a] Leandro Gomes Silva e Silva,[b] Hinnerk Bormann,[b] Michael Niedermeiser,[b] Dennis Haupt,[b] Ottmar Schläfer,[b] and Michael Sievers[b]

[a]*Clausthal University of Technology, Institute of Chemical and Electrochemical Process Engineering, D-38678 Clausthal-Zellerfeld, Germany*
[b]*Clausthal Research Center for Environmental Technologies, D-38678 Clausthal-Zellerfeld, Germany*

In this study, mixtures of graphite, γ-MnO_2 and MoS_2 with different weight proportions (20:1:1, 30:1:2 and 30:2:1) were used in microbial fuel cells (MFCs) and the catalysts were also subjected to ultrasonication to study its influence. The data suggest that the MFC fabricated with the catalyst prepared using graphite, γ-MnO_2 and MoS_2 in a weight proportion of 20:1:1 exhibited the highest optimal power density of 120 mW/m^2. However, after ultrasonic treatment, the power density was significantly improved, which was 183 mW/m^2. It can also be observed that after using ß-MnO_2, the optimal power density of the MFC fabricated with the catalyst prepared with graphite, ß-MnO_2 and MoS_2 in a proportion of 20:1:1 higher (158 mW/m^2) than that of the MFC fabricated with γ-MnO_2 in the same proportion, showing that the performance of ß-MnO_2 with a whisker structure was better than that of γ-MnO_2 owing to its higher surface area, larger pore diameter and great pore volume. The long term performances of the MFCs fabricated using catalysts prepared with the different graphite, γ-MnO_2 (ß-MnO_2) and MoS_2 proportions decreased finally in the order of 20:1:1 (ß-MnO_2) > 20:1:1 (ultrasonicated γ-MnO_2) > 10:1 (ß-MnO_2) >20:1:1 (γ-MnO_2) > 30:2:1 (γ-MnO_2) >30:1:2 (γ-MnO_2).

Manuscript submitted August 14, 2017; revised manuscript received November 7, 2017. Published December 2, 2017.

Recently, because of the increasing energy shortage and growing awareness of environmental protection, harvesting low-grade waste heat as electrical power has drawn a great deal of attention because of its potential and availability often at locations where electrical power is needed.[1–4] Hydraulic, wind and solar radiation are typical examples of clean energy resources used as alternatives to fossil fuel resources to produce electricity. However, these energy sources are limited by climate and geographical factors. When compared with the energy sources mentioned previously, biomass is one of the important renewable carbon sources and has been recognized as a promising energy supplier of the future.[5] The increasing demand for biofuel has encouraged researchers and politicians worldwide to find sustainable biofuel production systems in accordance with the regional conditions and needs.[6] Microbial fuel cells (MFCs) are bioelectrochemical devices used to generate electricity from organic matter using exoelectrogenic bacteria.[7] This technology shows promise in both wastewater treatment and sustainable bioenergy conversion applications.[8] In the MFC, electrons liberated from the degradation of the electrolyte organics move through the external circuit to the cathode where oxygen is reduced and a net current/power is generated.[9] It has be shown that the oxygen reduction reaction (ORR) at the cathode is one of the main limiting factors for further improving the output of MFCs.[10,11]

An improvement in the cathodic process can lead to a considerable power density increases in MFCs.[12] One of the solutions is to add catalyst on the surface of the cathode, in which Pt is a typical example. Pt-based catalysts are the best ORR catalysts, however, because of its high cost, it is necessary to study environmental friendly catalysts with lower price. Ideal ORR catalysts are generally used as the oxygen cathodes to reduce the overpotential and obtain more energy, and are usually based on metals, carbon, conductive polymers and microbes.[13] The potential electrochemical catalysts used for MFCs have to be widely available and should be low cost materials. Therefore, metal-based catalysts containing Co,[14,15] Fe,[16,17] Mn,[5,18,19] Cu,[20] and Ni[21] are recognized as promising ORR catalysts and have been heavily studied.

Suman et al. have used graphite felt and stainless steel assembly as cathode of microbial electrolysis cell (MEC) in the study of acetate production and achieved a maximum acetate production rate of 1.3 mM/day.[22] Atanassov et al.[23] compared the ORR catalysts based on Fe, Co, Ni and Mn with the same precursor (aminoantipyrine, AAPyr) using an identical sacrificial support method. The results showed that the power density of the MFC fabricated with these catalysts decreased in the order: Fe-AAPyr> Co-AAPyr> Ni-AAPyr>Mn-AAPyr> AC. The surface of transition metal oxides can favor electron localization over the bulk itinerant electron state, which improves the catalytic activity in the ORR.[24]

Manganese dioxide (MnO_2) is considered to be a promising cathode catalyst for alkaline fuel cells and metal-air batteries[25] because oxygen reduction activity can be achieved on MnO_2 in an alkaline media.[26] Recently, many studies[27] have focused on the effect of MnO_2 catalysts on improving the performance of the cathode in MFCs. Because of the low conductivity of MnO_2, major benefits can be achieved by anchoring MnO_2 nanostructures over carbon supports such as graphite, activated carbon (AC), carbon nanotube (CNT) and graphite oxide (GO). The carbon support (graphite) is expected to increase the electrochemically active surface area and number of active sites to improve the performance of MnO_2 catalysts.[28] Hu et al.[29] have developed manganese oxide catalysts using a cryptomelane-type octahedral molecular sieve (OMS-2) to replace the Pt catalyst in the cathode. They investigated undoped and three catalysts doped with cobalt (Co-OMS-2), copper (Cu-OMS-2) and cerium (Ce-OMS-2) to improve the catalytic performance. During the experiments, they found that the voltage of the Co-OMS-2 granular active carbon microbial fuel cell (GACMFC) was 217 mV and the power density was 180 mW/m^2, which was the highest among the other catalysts studied. The chemical oxygen demand (COD) removal efficiencies of the Cu-OMS-2 MFCs and Co-OMS-2 MFCs possessed values between 83% and 87%, which were 15–19% higher than that of Pt MFCs.[30] Furthermore, the Cu-OMS-2 MFCs and Co-OMS-2 MFCs possessed a stable power generation of 200 ± 8 mV and 190 ± 5 mV, respectively, which were 50–60 mV higher than that of Pt MFCs. Zhang et al.[31] developed MnO_2-coated electrodes for MFCs and achieved a power density of 3580 ± 130 mW/m^2, which was 24.7% higher than the MFC fabricated with bare carbon felt. Liu et al.[32] have also studied nano-structured manganese oxide as a cathodic catalyst for MFCs. They demonstrated that a nano-structured MnOx can be an effective catalyst for MFCs and produced a maximum power density of 772.8 mW/m^2 using synthetic wastewater. Jiang et al. have also developed a Co-MnO_2 cathode for MFCs and obtained a power density of 465 mW/m^2.[33] Our group[5] have reported graphite plus MnO_2 paints, which were used as the catalyst in a stainless steel cathode. We found that

[z]E-mail: bolong.jiang@tu-clausthal.de

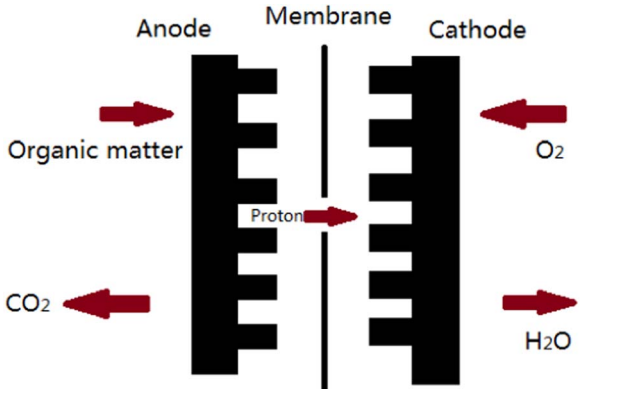

Figure 1. Schematic of the basic elements of single MFC.

the MFC fabricated with the cathode without the catalyst possessed a power density of ~40 mW/m^2, while the best MFC performance was obtained with the graphite/MnO_2 composite (10:1) with a power density of 100 mW/m^2, which showed that MnO_2 is a promising catalyst for improving the performance of MFCs with domestic wastewater. Roche et al.[34] developed a two chamber MFC using MnO_x/C as the catalyst in the cathode that was used to treat sewage sludge, whose results showed that the power density of the MFC fabricated with the MnO_x/C composite was 161 mW/m^2. When compared with the MFC fabricated with Pt/C, its power density was only 19.8% lower than that of MFC fabricated with Pt/C (193 mW/m^2).

Another alternative catalyst, which has recently attracted a great deal of attention is molybdenum sulfide (MoS_2).[5] Because of its high stability, MoS_2 is usually unaffected by dilute acids and oxygen. Yuan et al.[35] have studied the effect of highly conductive carbon nanotubes (CNT) with a MoS_2 coating on the performance of microbial electrolysis cells used for the hydrogen evolution reaction. They found that the hydrogen evolution reaction activity of the MoS_2/CNT composite was comparable to that of Pt. Hou et al.[36] have also developed a MoS_2/nitrogen-doped graphene nanosheet aerogels catalyst for hydrogen evolution in an MEC. They achieved a high output current density of 0.36 mA/cm^2. Furthermore, a hydrogen production rate of 19 m^3/day was also obtained for the hybrid at a bias of 0.8 V. Our group[5] have also shown that the graphite/MoS_2 composite shows a much higher stability than the graphite/MnO_2 composite.

In this study, oxygen reduction catalysts comprised of graphite, MnO_2 and MoS_2 at different weight proportions were prepared and the effects of the weight proportion and ultrasonic treatment on the performance of MFC were studied. In addition, to further investigate the effect of different MnO_2 morphologies and structure on the performance of the MFCs, ß-MnO_2 with a whisker structure was also prepared and used as a oxygen reduction catalyst in an MFC. A reversible reference electrode was also used in our experiments to measure the potential of the single electrodes, in order that the performance of the cathode and anode can be compared with each other.

Materials and Methods

Design of MFC.—A schematic of the used MFC with anode dimension of 150 mm × 150 mm is shown in Fig. 1. The system was designed to keep the bacteria on the anode separated from the cathode solution, which can be realized by using a membrane or separator. Moreover, the separator should also be used for proton exchange. During the experiments proton exchange membranes were used as separator between anode and cathode compartment of the MFCs. Polymer/graphite composite is used as material of flat plate electrodes, which are prepared by Eisenhuth Corporation (Germany) (Fig. 2).

Figure 2. Construction of anode plate.

Preparation of graphite/MnO_2 and graphite/MoS_2 composite.—For preparing the cathode dispersion, MnO_2 was received by Guangzhou Chun Zheng Chemical Corporation in China, MoS_2 by Metallpulver24 Corporation in Germany (article number 22020) and graphite RA by Eisenhuth Corp. Germany.

New form of MnO_2 (ß-MnO_2) catalyst is also studied in our research, which was prepared according to the method of Zhang et al.[37] In which, $KMnO_4$, ethanol and water were mixed together and then sealed and maintained at 125°C for 24 h before cooling down to room temperature. After washed and dried, the precipitates were calcined at 300°C for 5 h. The catalyst was cooled to room temperature before putting into use.

Graphite, MnO_2 and MoS_2 are mixed in a weight proportion of 20:1:1, 30:1:2 and 30:2:1 respectively. As a polymer binder a solution made of 150 mL butanol and 7.5 g celluloid (taken from table tennis balls) is produced. The mixture of MnO_2, MoS_2 and graphite is added into the butanol solution. The components were chosen considering the aspect that no poisonous materials should be used in a water treatment plant. In our research, the catalysts were coated by paintbrush on the surface of cathode with the average loading ratio of 0.16 g (catalyst)/g (cathode). In order to study the influence of ultrasonic treatment on the performance of MFC, graphite, MnO_2 and MoS_2 which are mixed in a weight proportion of 20:1:1 are also treated under ultrasonication for 30 min. Stainless steel meshes (w = 1.8 mm, d = 0.32 mm) from Spörl KG Präzisionsdrahtweberei Corporation (Germany) with dimension of 150 mm × 150 mm were used as cathode. A sample of a stainless steel cathode with graphite/MnO_2 composite coating and four in series connected MFCs with stainless steel as cathode carrier material is given in Fig. 3.

Measurement of power density.—State of the art in MFC research is the use of resistors with fixed values as an electric load, which is also described in our previous research. The resistor is needed to allow the microorganism to release their generated electrons. This method however, is not the best approach to load the MFCs electrically. MFCs are electrochemical reactors with living organism on the electrodes. This results in fluctuations of power density which cannot be forecast. Therefore a fixed resistor does not fit optimal to the variable power output of the MFC. The stronger the ability of microorganism to produce electron is, the longer their vitality is and the better the bio-film on electrode can develop. Our approach in the research is different from the well-known resistor load. The MFCs are loaded with constant current sources. The current is adapted to the prevailing power capability of the MFC. By this means, the MFCs were loaded individually with different constant currents, each MFC is connected

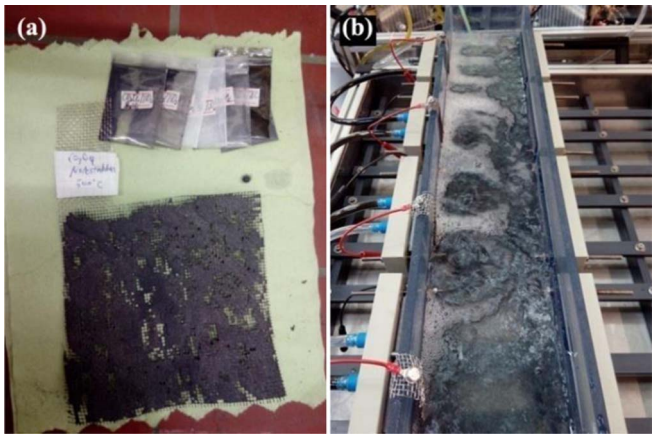

Figure 3. Stainless steel mesh with catalyst (a) and four in series connected MFCs (b).

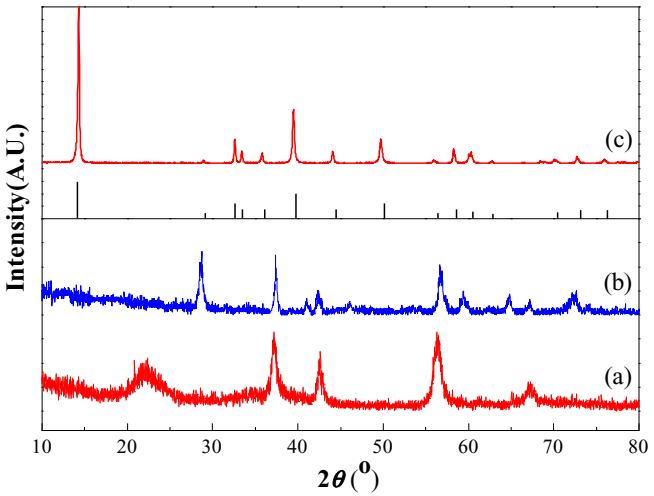

Figure 4. XRD patterns of the purchased γ-MnO_2 (a), as-prepared ß-MnO_2 (b) and MoS_2 (c) catalysts.

with an own constant current source. Simultaneously the potential was measured. The current density-voltage and the current density-power density characteristics can be further calculated automatically by LabView software combining with these measured data (National Instruments). These data are not constant over time but change during the operation of a MFC, which is caused by changing supply with nutrition, varying supply with oxygen and individual development of the microbial film on the electrodes. So it is necessary to measure these data several times a day and adjust the applied load current to the maximum power point in the current density/power density characteristic of each MFC. By comparing the latest voltage and current with the stored previous data, the status of operation is identified.

The current is then adjusted stepwise toward the direction of the power maximum. The time interval for the measurements can be chosen freely as well as the current increments, so this method can be adapted to different sizes of MFCs. By this approach each MFC was operated at the individual maximum power point in the current density/power density characteristic and a rapid development of the microorganism could be reached leading to a fast power production. Materials with beneficial properties can be easily detected and be used for the development of industrial MFCs. The performance of different materials can be compared and evaluated at their maximum power point by this method.[5]

Characterization.—The X–ray powder diffraction (XRD) analysis were recorded on a D/max-2200PC-X-ray diffractometer (40 kV, 20 mA) using CuKα radiation (0.15404 nm), scan range from 10 to 80° at a rate of 10°/min. The typical physico-chemical properties of supports and catalysts were analyzed by BET method using Micromeritics adsorption equipment of NOVA2000e. All the samples were outgassed at 200°C until the vacuum pressure was 6 mm Hg. The morphological and surface composition characterization of the samples were obtained using scanning electron microscopy (SEM, NOVA600, FEI) and energy dispersive X-ray spectrometry (EDS).

Results and Discussion

Characterization of MnO_2 and MoS_2.—XRD patterns were used to identify and confirm the crystalline phases of samples used as catalysts (Fig. 4). It can be observed from Fig. 4 that for purchased γ-MnO_2, the peaks at 2θ = 22.3°, 37.1°, 42.4°, 56.6°, 65.7° and 67.3° (PDF: 03–0953) can be seen, which confirmed that the purchased MnO_2 sample was γ-MnO_2. For as-prepared β-MnO_2, the peaks at 2θ = 28.7°, 37.3°, 41.0°, 42.8°, 46.1°, 56.7°, 59.4°, 64.8°, 67.2°, 68.6°, 72.3° and 72.4° can be seen, which confirmed that the prepared MnO_2 sample was β-MnO_2. For MoS_2, the sharp peaks at 2θ = 14.4°, 29.0°, 32.7°, 33.5°, 35.9°, 39.5°, 44.2°, 49.8°, 56.0°, 58.3°, 60.1°, 62.8°, 70.1°, 72.8° and 76.0° (PDF: 37–1492) can clearly be seen, which confirmed that the sample was MoS_2 of good crystallinity.

Table I shows the textural properties of different catalysts. It can be observed from Table I that the surface area, pore volume and diameter of γ-MnO_2 were 57.1 $m^2 \cdot g^{-1}$, 0.072 $cm^3 \cdot g^{-1}$ and 4.9 nm, respectively. While for ß-MnO_2, the surface area, pore volume and diameter were 68.3 $m^2 \cdot g^{-1}$, 0.281 $cm^3 \cdot g^{-1}$ and 16.5 nm, respectively. This shows that the ß-MnO_2 possessed a higher surface area than that of γ-MnO_2. In addition, the pore diameter and pore volume of ß-MnO_2 were 2.9 times and 2.4 times larger than those of γ-MnO_2, respectively. The above results showed that the structures of the γ-MnO_2 and ß-MnO_2 catalysts were significantly different even though their compositions are the same. The ß-MnO_2 is more likely to be a better catalyst than γ-MnO_2 owing to its textural properties. This will further discussed later. For MoS_2, the surface area, pore volume and diameter were 7.7 $m^2 \cdot g^{-1}$, 0.038 $cm^3 \cdot g^{-1}$ and 19.2 nm, respectively. Comparing with γ-MnO_2 and ß-MnO_2, the MoS_2 catalyst possessed a lower surface area with a relatively low pore volume.

Fig. 5 illustrates SEM morphologies of the γ-MnO_2, MoS_2 and ß-MnO_2 catalysts. It can be observed from Fig. 5 that γ-MnO_2 catalyst showed an irregular form and rough edges (Fig. 5a). The morphologies of the γ-MnO_2 and ß-MnO_2 catalysts are significantly different. The ß-MnO_2 catalyst clearly maintains the whisker structure (Fig. 5c). Comparing with those MnO_2 catalysts, the morphology of MoS_2 catalyst (Fig. 5b) is much more regular with several layers.

Polarization curves of MFC with different catalysts.—The power density performance of MFCs with different graphite, γ-MnO_2 and MoS_2 proportion is shown in Fig. 6 (left). The data suggested that the optimal power densities of MFCs with catalysts prepared by graphite, γ-MnO_2 and MoS_2 in a proportion of 30:1:2 and 30:2:1 were lower than 60 mW/m^2. The MFC fabricated with a catalyst prepared by graphite, γ-MnO_2 and MoS_2 in a proportion of 20:1:1 possessed the highest optimal power density of 120 mW/m^2. This value is two times the optimal power of the MFCs fabricated using the catalysts prepared by graphite, γ-MnO_2 and MoS_2 in a proportion of 30:1:2 and 30:2:1.

Table I. Textural properties of γ-MnO_2, MoS_2 and ß-MnO_2 catalysts.

Sample	$S_{BET}/(m^2 \cdot g^{-1})$	$V_p/(cm^3 \cdot g^{-1})$	D/(nm)
γ-MnO_2	57.1	0.072	4.9
β-MnO_2	68.3	0.281	16.5
MoS_2	7.7	0.038	19.2

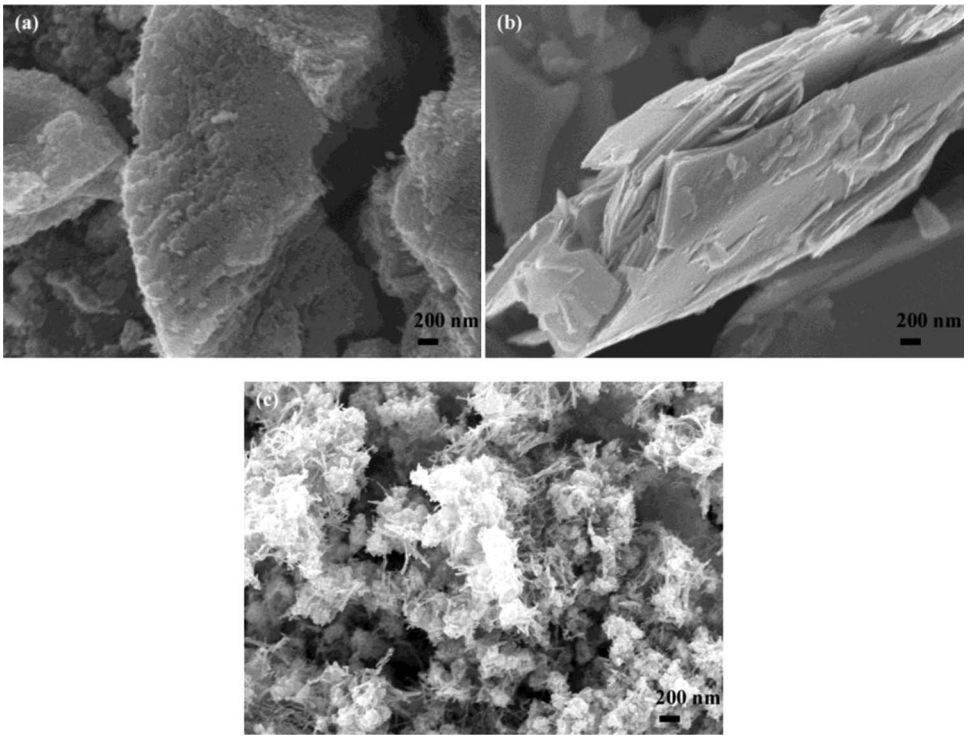

Figure 5. SEM morphologies of γ-MnO_2 (a), MoS_2 (b) and ß-MnO_2 (c) catalysts.

This shows that the proportion of graphite has significant effect on the power density. A RHE is also used in our experiments for measuring the potential of single electrode and the data is shown in Fig. 6 (right). The similar results were obtained. It can be seen that the cathode potential of MFC fabricated with a catalyst prepared by graphite, γ-MnO_2 and MoS_2 in a proportion of 20:1:1 descended slower than those of MFCs with other mixing proportions. The main reason is that the MFC fabricated with a catalyst prepared by graphite, γ-MnO_2 and MoS_2 in a proportion of 20:1:1 possesses the highest optimal power density.

The influence of ultrasonic treatment on the performance of power density of MFC is shown in Fig. 7. The data suggested that the MFC fabricated with a catalyst prepared by graphite, γ-MnO_2 and MoS_2 in a proportion of 20:1:1 with ultrasonic treatment possessed a significantly higher power density (183 mW/m^2) than the one without ultrasonic treatment, showing that ultrasonic treatment plays an important role in improving the power density of MFC. The possible reason maybe that the ultrasonic treatment can promote a good mix of the graphite, γ-MnO_2 and MoS_2, and therefore can produce more uniform composite. This would play positive role in energy production. Sang et al.[38] have pretreated different sludge types for MFC and found that the ultrasonic pretreatment have changed the physical structure of sludge and therefore, a higher electricity production was obtained.

The influence of different MnO_2 morphologies on the performance of power density of MFC is shown in Fig. 8. The data suggested that the optimal power density of MFC fabricated with a catalyst prepared from graphite and ß-MnO_2 in a proportion of 10:1 was 140 mW/m^2, which is higher than that of MFC fabricated with a catalyst prepared

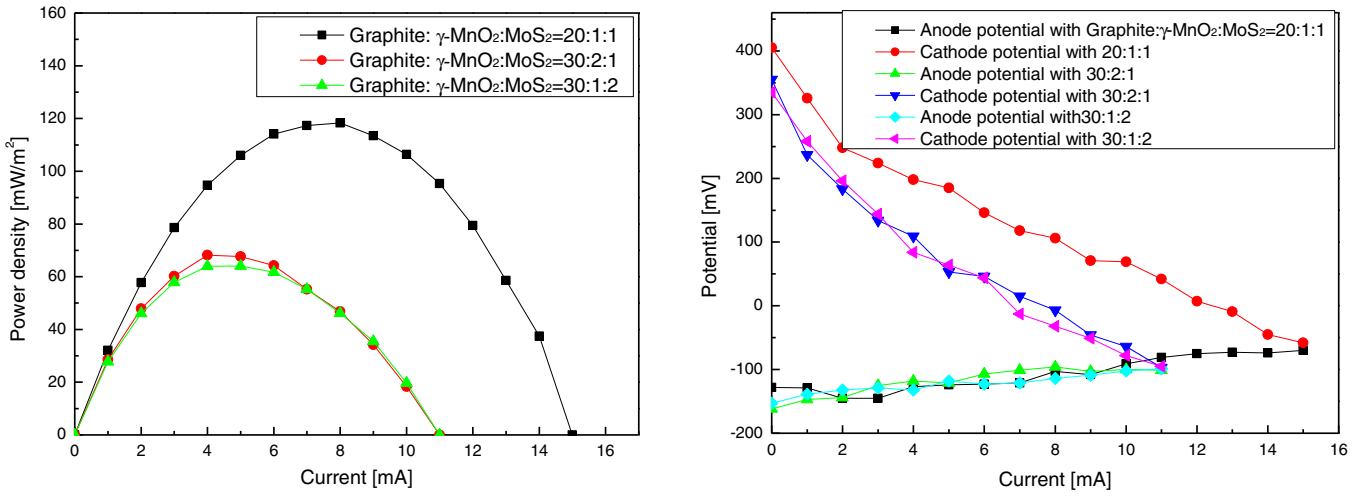

Figure 6. Power densities of MFCs with cathodes based on the catalysts prepared using graphite, γ-MnO_2 and MoS_2 in different proportions as indicated (left) and the corresponding potential measurement (right).

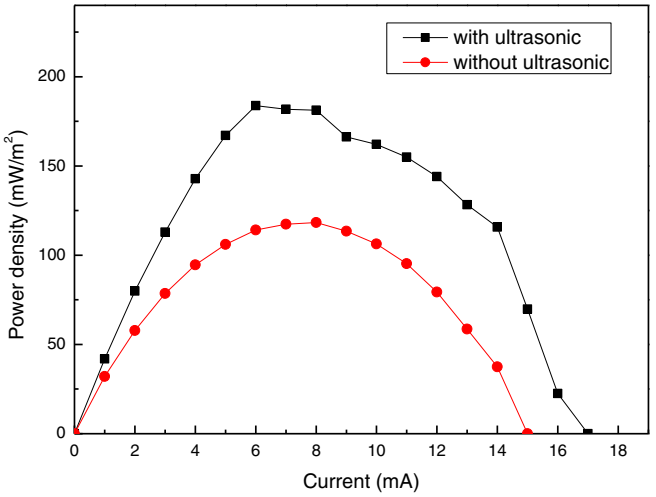

Figure 7. Power densities of MFCs with cathodes based on the catalyst prepared using graphite, γ-MnO_2 and MoS_2 in a proportion of 20:1:1 with and without ultrasonic treatment.

form graphite, γ-MnO_2 and MoS_2 in a proportion of 20:1:1, showing that the performance of ß-MnO_2 with a whisker structure was much better than γ-MnO_2. This can be attributed to the higher surface area, larger pore size and great pore volume of ß-MnO_2 (Table I). It should be noted that the higher surface area is beneficial to expose more active sites, which would enhance the catalytic performance. While the larger pore diameter and pore volume would facilitate the diffusion rates of the reactant, which is beneficial toward chemical reactions over the catalysts. Furthermore, the average oxidation state (AOS) of manganese oxide would also play a role in the performance. Shen et al.[39] have measured the AOS value of different manganese oxide samples via a magnetic method and found that the ß-MnO_2 possessed the highest AOS value (4.23) comparing with γ-MnO_2 (4.04). Zhang et al.[37] have tested three manganese dioxide materials, α-MnO_2, ß-MnO_2, γ-MnO_2 as cathodic catalysts in air-cathode MFCs and found that ß-MnO_2 appeared to hold the highest catalytic activity. They concluded that the high catalytic activity of ß-MnO_2 is due to its high BET surface and AOS value. Comparing with MFC fabricated with a catalyst prepared from graphite and ß-MnO_2 in a proportion of 10:1, the MFC fabricated with a catalyst prepared from graphite, ß-MnO_2 and MoS_2 in a proportion of 20:1:1 possessed even a higher power density, which is 158 mW/m^2. This indicated that addition of MoS_2 is beneficial to enhance the MFC performance.

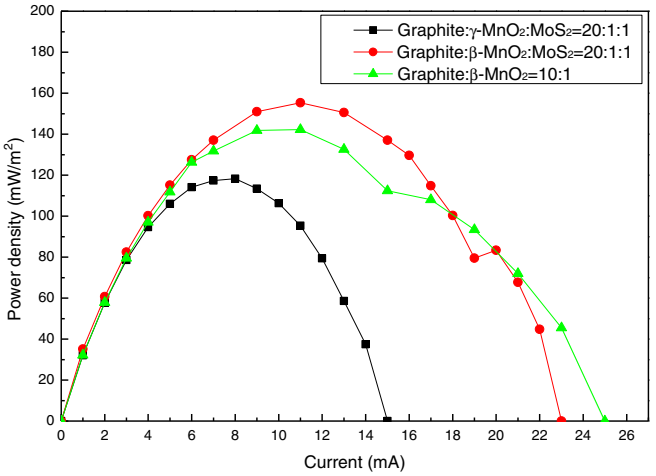

Figure 8. Power densities of MFCs with cathodes based on the catalysts prepared using graphite, ß-MnO_2 (γ-MnO_2) and MoS_2.

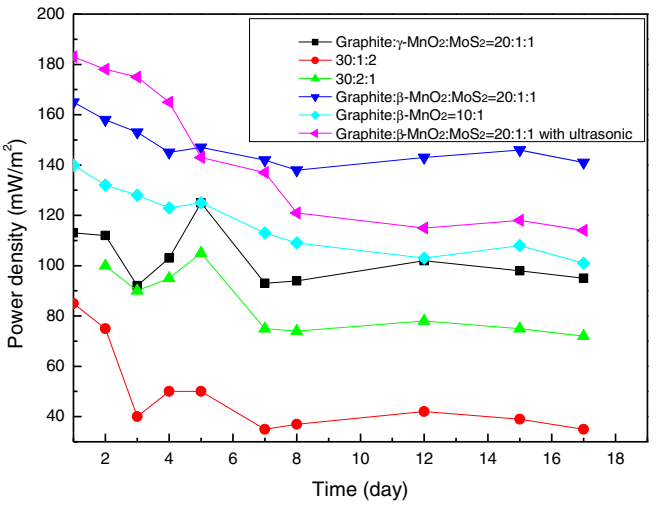

Figure 9. Long term performances of MFCs with cathodes based on the catalysts prepared using graphite, ß-MnO_2 (γ-MnO_2) and MoS_2 in different proportions.

Long term performance of MFC fabricated with a catalyst prepared by different proportions.—The long term performance of MFCs with catalysts prepared with different graphite, γ-MnO_2 (ß-MnO_2) and MoS_2 proportions is shown in Fig. 9. The data suggested that for all the samples, the power densities became stable after 12th day and a slight descend is observed. The MFC fabricated with the catalyst prepared from graphite, γ-MnO_2 and MoS_2 in a proportion of 20:1:1 achieved the highest power density of 125 mW/m^2 on 5th day. The power density of MFC fabricated with a catalyst prepared from graphite, γ-MnO_2 and MoS_2 in a proportion of 30:1:2 possessed the value of only 85 mW/m^2 at the beginning and descended rapidly after starting operation. However, after 12th day, the power density of MFC fabricated with a catalyst prepared from graphite, γ-MnO_2 and MoS_2 in a proportion of 20:1:1 fluctuated around the value of 95 mW/m^2, which is still much higher than those of MFCs catalysts prepared from graphite, γ-MnO_2 and MoS_2 in proportions of 30:1:2 (35 mW/m^2) and 30:2:1 (75 mW/m^2). This demonstrated that among the MFC fabricated with a catalysts prepared from different graphite, ß-MnO_2 and MoS_2 proportions, the MFC fabricated with a catalyst prepared from graphite, ß-MnO_2 and MoS_2 in a proportion of 20:1:1 showed the highest power density.

The power density of MFC fabricated with a catalyst prepared from graphite, ß-MnO_2 in a proportion of 10:1 is 140 mW/m^2 on the 1st day, which is better than those of MFC fabricated with a catalyst prepared from graphite, γ-MnO_2 and MoS_2 combinations. While the MFC fabricated with a catalyst prepared from graphite, ß-MnO_2 and MoS_2 in a proportion of 20:1:1 showed the power density of 165 mW/m^2 on the 1st day, and fluctuated around the value of 142 mW/m^2, which is the highest among all the tested combinations. This observation agrees well with the results of power densities analysis described above (Fig. 9), which indicated that the performance of crystallized ß-MnO_2 is much better than γ-MnO_2. However, it can also be observed that the power density of The MFC fabricated with a catalyst prepared from graphite, γ-MnO_2 and MoS_2 in a proportion of 20:1:1 with ultrasonic treatment possessed the highest power density only at the first 4 days. After 4 days, the power density became lower and possessed the value of 114 mW/m^2 on the 17th day.

It can be observed in Fig. 9 that almost all the power densities with different catalysts have descended with time and fluctuated around a certain value. This phenomenon is also observed in our previous research.[5] We used the mixture of graphite and MnO_2 with proportion of 10:1. The data suggested that because of the growth of microorganism, the power density increased rapidly at the beginning. However, the power density decreased and fluctuated around a value, which is

lower than the highest value in the long term performance. This phenomenon could be attributed to both the degradation of microorganism on the anode side and deactivation of catalysts because of chemical reaction for a long time. This observation is in accordance with results obtained by Zhou et al.[40] They have developed a MFC stack and investigated the long term behavior of power density for 180 days. They showed that after 30 days, the power density decreased from 4 W/m^3 to 1.5 W/m^3 within 150 days, which was stable. The long term performances of the MFCs fabricated using catalysts prepared with the different graphite, γ-MnO_2 (ß-MnO_2) and MoS_2 proportions were decreased in the order of 20:1:1 (ß-MnO_2) > 20:1:1 (ultrasonicated γ-MnO_2) >10:1 (ß-MnO_2) >20:1:1 (γ-MnO_2) > 30:2:1 (γ-MnO_2) >30:1:2 (γ-MnO_2).

Conclusions

Mixtures of graphite, γ-MnO_2 and MoS_2 at different weight proportions (20:1:1, 30:1:2 and 30:2:1) were prepared and used as oxygen reduction catalysts in MFCs. To further investigate the effect of different MnO_2 morphologies on the MFC performance, ß-MnO_2 with a whisker structure was also prepared. It was observed that among the graphite, γ-MnO_2 and MoS_2 combinations, the MFC fabricated with the catalyst prepared from graphite, γ-MnO_2 and MoS_2 in a proportion of 20:1:1 possessed the highest optimal power density of 120 mW/m^2, which was two times the optimal power of the MFCs fabricated using the catalysts prepared with graphite, γ-MnO_2 and MoS_2 in proportions of 30:1:2 and 30:2:1. When compared with the graphite, γ-MnO_2 and MoS_2 combination, the optimal power density of the MFC fabricated with a catalyst prepared using graphite, ß-MnO_2 and MoS_2 in a proportion of 20:1:1 was higher (158 mW/m^2), showing that the performance of ß-MnO_2 with a whisker structure was much better than that of γ-MnO_2 owing to its higher surface area, larger pore diameter and great pore volume. Furthermore, the ß-MnO_2 possessed a higher oxidation state than γ-MnO_2, which is also an important reason for better performance of ß-MnO_2.

For long term performance, the MFC fabricated using the catalyst prepared with graphite, ß-MnO_2 and MoS_2 in a proportion of 20:1:1 possessed a power density of 165 mW/m^2 on the 1st day, which fluctuated at ∼142 mW/m^2 and was the highest among all the combinations tested. This observation agrees well with the power density analysis described previously (Fig. 8), which indicates that the performance of crystallized ß-MnO_2 was much better than γ-MnO_2. During the long term performance, the MFC with 20:1:1 (ultrasonicated γ-MnO_2) possessed the highest power density at beginning. However, it began to decrease significantly after 4th day and became lower than that of MFC with 20:1:1 (ß-MnO_2). The long term performances of the MFCs fabricated using catalysts prepared with the different graphite, γ-MnO_2 (ß-MnO_2) and MoS_2 proportions were decreased finally in the order of 20:1:1 (ß-MnO_2) > 20:1:1 (ultrasonicated γ-MnO_2) > 10:1 (ß-MnO_2)>20:1:1 (γ-MnO_2) > 30:2:1 (γ-MnO_2) > 30:1:2 (γ-MnO_2). This reveals that the catalyst prepared using graphite, ß-MnO_2 and MoS_2 in a proportion of 20:1:1 was optimal.

References

1. Y. Kim, S. Yamanaka, A. Nakajima, and T. Ogawa, *Adv. Energy Mater.*, **5**, 6 (2015).
2. A. P. Straub, N. Y. Yip, S. Lin, and J. Lee, *Nat. Energy*, **1**, 16090 (2016).
3. A. Carati, M. Marino, and D. Brogioli, *Energy*, **93**, 984 (2015).
4. X. Niu, J. L. Yu, and S. Z. Wang, *J. Power Sources*, **188**, 621 (2009).
5. B. Jiang, T. Muddemann, U. Kunz, H. Bormann, M. Niedermeiser, D. Haupt, O. Schläfer, and M. Sievers, *J. Electrochem. Soc.*, **164**, H3083 (2017).
6. D. Rathore, A. S. Nizami, A. Sing, and D. Pant, *Biofuel Res. J.*, **3**, 380 (2016).
7. X. Zhang, W. He, L. Ren, J. Stager, P. J. Evans, and B. E. Logan, *Bioresour. Technol.*, **176**, 23 (2015).
8. S. Beenish, A. D. Christy, Z. Yu, and C. Anne, *Renew. Sustain. Energy Rev.*, **73**, 75 (2017).
9. H. Yuan, Y. Hou, I. M. A. Reesh, J. Chen, and Z. He, *Mater. Horiz.*, **3**, 382 (2016).
10. H. Y. Wang, G. M. Wang, Y. C. Ling, F. Qian, Y. Song, X. H. Lu, S. W. Chen, Y. X. Tong, and Y. Li, *Nanoscale*, **5**, 10283 (2013).
11. H. Rismani-Yazdi, S. M. Carver, A. D. Christy, and O. H. Tuovinen, *J. Power Sources*, **180**, 683 (2008).
12. W. He, W. Yang, Y. Tian, and X. Zhu, *Journal of Power Sources*, **332**, 447 (2016).
13. Z. Wang, C. Cao, Y. Zheng, S. Chen, and F. Zhao, *Chem Electro Chem*, **1**, 1813 (2014).
14. B. Liu, C. Brückner, Y. Lei, Y. Cheng, C. Santoro, and B. Li, *J. Power Sources*, **257**, 246 (2014).
15. F. Zhao, F. Harnisch, U. Schröder, F. Scholz, P. Bogdanoff, and I. Herrmann, *Electrochem. Commun.*, **7**, 1405 (2005).
16. M. T. Nguyen, B. Mecheri, A. D. Epifanio, T. P. Sciarria, F. Adani, and S. Licoccia, *Int. J. Hydrogen Energy*, **39**, 6462 (2014).
17. M. T. Nguyen, B. Mecheri, A. Iannaci, A. D. Epifanio, and S. Licoccia, *Electrochim. Acta*, **190**, 388 (2016).
18. E. Martin, B. Tartakovsky, and O. Savadogo, *Electrochim. Acta*, **58**, 58 (2011).
19. P. Zhang, K. Li, and X. Liu, *J. Power Sources*, **264**, 248 (2014).
20. M. Ghasemi, W. Daud, M. Rahimnejad, M. Rezayi, and A. Fatemi, *Int J Hydrogen Energy*, **38**, 9533 (2013).
21. J. Huang, N. Zhu, T. Yang, T. Zhang, P. Wu, and Z. Dang, *Biosens. Bioelectron.*, **72**, 332 (2015).
22. B. Suman, H. Annemiek, and B. Xochitl, *Bioresource Technology*, **195**, 14 (2015).
23. K. Mounika, S. Carlo, S. Alexey, K. Sadia, A. Kateryna, M. Ivana, and A. Plamen, *Electrochimica. Acta.*, **231**, 115 (2017).
24. J. Suntivich, H. A. Gasteiger, N. Yabuuchi, H. Nakanishi, J. B. Goodenough, and Y. Shao-Horn, *Nat. Chem.*, **3**, 546 (2011).
25. Z. D. Wei, W. Z. Huang, S. T. Zhang, and J. Tan, *J. Power Sources*, **91**, 83 (2000).
26. F. Lima, M. L. Calegaro, and E. A. Ticianelli, *J. Electroanal. Chem.*, **590**, 152 (2006).
27. D. Zhang, D. Chi, T. Okajima, and T. Ohsaka, *Electrochim. Acta.*, **52**, 5400 (2007).
28. E. Antolini, *Biosens. Bioelectron.*, **69**, 54 (2015).
29. X. Li, B. Hu, St. Suib, Y. Lei, and B. Li, *J. Power Sources*, **195**, 2586 (2010).
30. X. Li, B. Hu, St. Suib, Y. Lei, and B. Li, *Biochem. Eng. J.*, **54**, 10 (2011).
31. Z. Changyong and L. Peng, *J. Power Sources*, **273**, 580 (2015).
32. L. Xianwei, S. Xuefei, and H. Yuxi, *Water research*, **44**, 5298 (2010).
33. D. Jiang, M. Curtis, and E. Troop, *Int. J. Hydrogen Energy*, **36**, 876 (2011).
34. I. Roche, K. Katuri, and K. Scott, *J. Appl. Electrochem.*, **40**, 13 (2010).
35. H. Yuan, J. Li, and C. Yuan, *Chem. Electro. Chem.*, **1**, 1828 (2014).
36. H. Yang, Z. Bog, and W. Zhenhai, *J. Mater. Chem. A.*, **2**, 13759 (2014).
37. L. Zhang, C. Liu, and L. Zhuang, *Biosens. Bioelectron.*, **24**, 2825 (2009).
38. S. Oh, J. Yoon, and A. Gurun, *Bioresour. Technol.*, **165**, 21 (2014).
39. X. Shen, Y. Ding, J. Liu, Z. Han, J. I. Budnick, W. A. Hines, and S. L. Suib, *J. Am. Chem. Soc.*, **127**, 6166 (2005).
40. S. Zhou, L. Zhuang, Y. Yuan, and Y. Wang, *Bioresour. Technol.*, **123**, 406 (2012).